Geomechanics and Engineering, *Vol. 32, No. 3 (2023) 293-305*
https://doi.org/10.12989/gae.2023.32.3.293

Impact of MJS treatment and artificial freezing on ground temperature variation: A case study

Jiling Zhao[1a], Ping Yang*[1], Lin Li[1], Junqing Feng[2] and Zipeng Zhou[3]

[1]*College of Civil Engineering, Nanjing Forestry University, Nanjing 210037, Jiangsu, China*
[2]*East China Construction Co., Ltd of China Railway No.3 Group. Nanjing, 211106, Jiangsu, China*
[3]*Nanjing Institute of Surveying, Mapping & Geotechnical Investigation, Co., Ltd. Nanjing 210019, Jiangsu, China*

(*Received October 14, 2022, Revised December 29, 2022, Accepted January 13, 2023*)

Abstract. To ensure the safety of underground infrastructures, ground can sometimes be first treated by cement slurry and then stabilized using artificial ground freezing (AGF) technique before excavation. The hydration heat produced by cement slurry increases the soil temperature before freezing and results in an extension of the active freezing time (AFT), especially when the Metro Jet System (MJS) treatment is adopted due to a high cement-soil ratio. In this paper, by taking advantage of an on-going project, a case study was performed to evaluate the influence of MJS and AGF on the ground temperature variation through on-site measurement and numerical simulation. Both on-site measurement and simulation results reveal that MJS resulted in a significant increase in the soil temperature after treatment. The ground temperature gradually decreases and then stabilized after completion of MJS. The initiation of AGF resulted in a quick decrease in ground temperature. The ground temperature then slowly decreased and stabilized at later freezing. A slight difference in ground temperature exists between the on-site measurements and simulation results due to limitations of numerical simulation. For the AGF system, numerical simulation is still strongly recommended because it is proven to be cost-effective for predicting the ground temperature variation with reasonable accuracy.

Keywords: active freezing time; artificial ground freezing; hydration heat; metro jet system; numerical simulation

1. Introduction

In megacities, a networked underground railway system is highly preferable to reduce surface traffic congestion. Different from surface transportation, intersection is not an option for underground subway. A new subway line to be constructed has to under- or over-pass existing subway lines/subway stations (e.g., Russo *et al.* 2015, Qi *et al.* 2022, Hu *et al.* 2021). Usually, an underpass by a subway line is not expected during the planning and construction of an underground structure. As a result, excavation for a new subway line has to should be made beneath the existing underground structure in this situation. Owing to excavation, existing structures are prone to a potential settlement (Liu *et al.* 2022). Therefore, before excavating, it is necessary to reinforce/stabilize the soil influenced by tunnel construction. Several methods such as jet grouting (e.g., Tonon 2011, Chen and Yang 2021), artificial ground freezing (e.g., Vitel *et al.* 2015, Francesca *et al.* 2016, Fan and Yang 2019, Yang *et al.* 2021), MJS (e.g., Chen *et al.* 2018, Zhang *et al.* 2018), pipe-roof (e.g., Liu *et al.* 2018, Shi *et al.* 2017), and underpinning of pile foundation (e.g., Yan *et al.* 2018, Wang *et al.* 2021) can be adopted for ground improvement. Among these methods, MJS and AGF are increasingly popular in underground projects.

The MJS treatment provides the required soil strength throughout the construction process. The frozen soil wall produced by AGF not only increases the soil ability in water-proof, which is considered to be critical for excavation of soil under a high pore-water pressure, but also further improves the soil bearing capacity. In addition, the frost heave during AGF process is reduced to a negligible level since the soil is already cement stabilized. This is the reason why the MJS and AGF are sometimes combined to reinforce/stabilize the soil around underground structures for very critical underground projects as addressed in a previously published paper (i.e., Zhao *et al.* 2020). To facilitate further construction, the formation of a frozen soil (i.e., soil temperature below 0 ^{o}C is considered the frozen soil) curtain is expected. Ground temperature distribution during freezing reveals the progression of frozen soil curtain formation. Consequently, ground temperature variation/monitoring is critical for the implementation of AGF technique. Numerous research efforts have been dedicated to investigating the ground temperature variation during artificial ground freezing (e.g., Levin *et al.* 2021, Lackner *et al.* 2005, Vasilyeva *et al.* 2019, Tounsi *et al.* 2020). In these studies, different influencing factors such as the seepage flow (Marwan *et al.* 2016, Huang *et al.* 2018), thermal conductivity (Huang *et al.* 2021, Li *et al.* 2020, Li *et al.* 2022), initial ground temperature (Fu *et al.* 2021), were analyzed and a coupled model considering these factors has been developed.

*Corresponding author, Professor
E-mail: yangping@njfu.edu.cn
[a]Ph.D. Student
E-mail: zhaojiling@njfu.edu.cn

ISSN: 2005-307X (Print), 2092-6219 (Online)

(a) Location (b) Cross section

Fig. 1 Location and cross section of the construction site (units: m)

The MJS technique is usually associated with a high cement-soil ratio and releases a large amount of heat during hydration. This will inevitably result in an increase in ground temperature before freezing. Consequently, the hydration heat from an MJS treatment can result in an extension of the active freezing time. The influence of hydration heat played an important role in influencing the soil temperature variation during freezing according to Fu *et al.* (2021). The main difference between the numerical model used in this paper and other existing models is the simulation in this paper is divided into two steps which includes the temperature variations due to the release of hydration heat (i.e., the construction for some MJS piles with similar construction time was accomplished at the same time) and artificial ground freezing process (i.e., taking the hydration heat temperature field as the initial temperature field of freezing). In existing models, the influence of cement-soil hydration heat is not taken into consideration in the simulation for soil temperature variation during artificial freezing (e.g., Levin *et al.* 2021, Tounsi *et al.* 2020).

Zhao *et al.* (2020) conducted a preliminary investigation to evaluate the effects of MJS hydration heat and other factors on the freezing temperature field through a numerical simulation. However, the setup for numerical simulation was not consistent with the on-site condition since it was made before the implementation of the MJS and AGF treatments. In this paper, by taking advantage of an ongoing project, the ground temperature variation under the influence of MJS treatment and AGF is investigated based on on-site measurement. A numerical simulation is also conducted under a setup (e.g., MJS layout, AGF layout, and calcium chloride brine temperature) consistent with the on-site condition. A comparison between the on-site measurement and numerical simulation was made to evaluate the rationality of numerical simulation.

2. Engineering background

2.1 Project overview

A new Metro Line (i.e., Line 7) was designed to underpass an existing subway station (i.e., Zhongsheng Station, Metro Line 10) in Nanjing, China. The location of Zhongsheng station is shown in Fig. 1(a). The distance between the roof of Metro Line 7 and floor of Zhongsheng Station is only 0.6 m, as schematically shown in Fig. 1(b). The soil under the influence of construction is mainly silty sand with a high water content. The ground water table is 2.60 ~ 3.20 m below the ground surface. The maximum water pressure encountered in this excavation zone is approximately 190 kPa. Considering the limited spacing of 0.6 m, any inappropriate reinforcement can potentially lead to a structure failure, surface subsidence, sand and water gushing, and settlement of surrounding buildings during excavation. Thus, the method of MJS + AGF was adopted for this ground improvement. To be specific, MJS treatment was implemented first, and the AGF was then performed to further strengthen the soil and improve the soil capability in water sealing. Meantime, MJS treatment was beneficial to reducing the frost heave from the AGF.

A preliminary numerical simulation by Zhao *et al.* (2020) reveals that the ambient temperature, insulation, hydration heat, and timing for initiation of freezing after MJS treatment play important roles in the ground temperature variation after the MJS treatment and initiation of AGF. The MJS and AGF were introduced for the ground improvement from 2020 to early 2021. However, significant differences exist between the system setups in the numerical simulation made in Zhao *et al.* (2020) and on-site construction. For example, as a very critical boundary condition, the air temperature applied in Zhao *et al*. (2020) was based on that in the year of 2019 instead of the actual time period from 2020 to early 2021. The construction scheme of soil reinforcement is significantly different from that in the previous numerical simulation. As a result, a new numerical simulation is conducted here to accurately re-evaluate the effect of hydration heat on temperature variation after the MJS treatment and initiation of AGF. A detailed comparison between in-situ measurement and numerical simulation is also made to verify the rationality of numerical simulation.

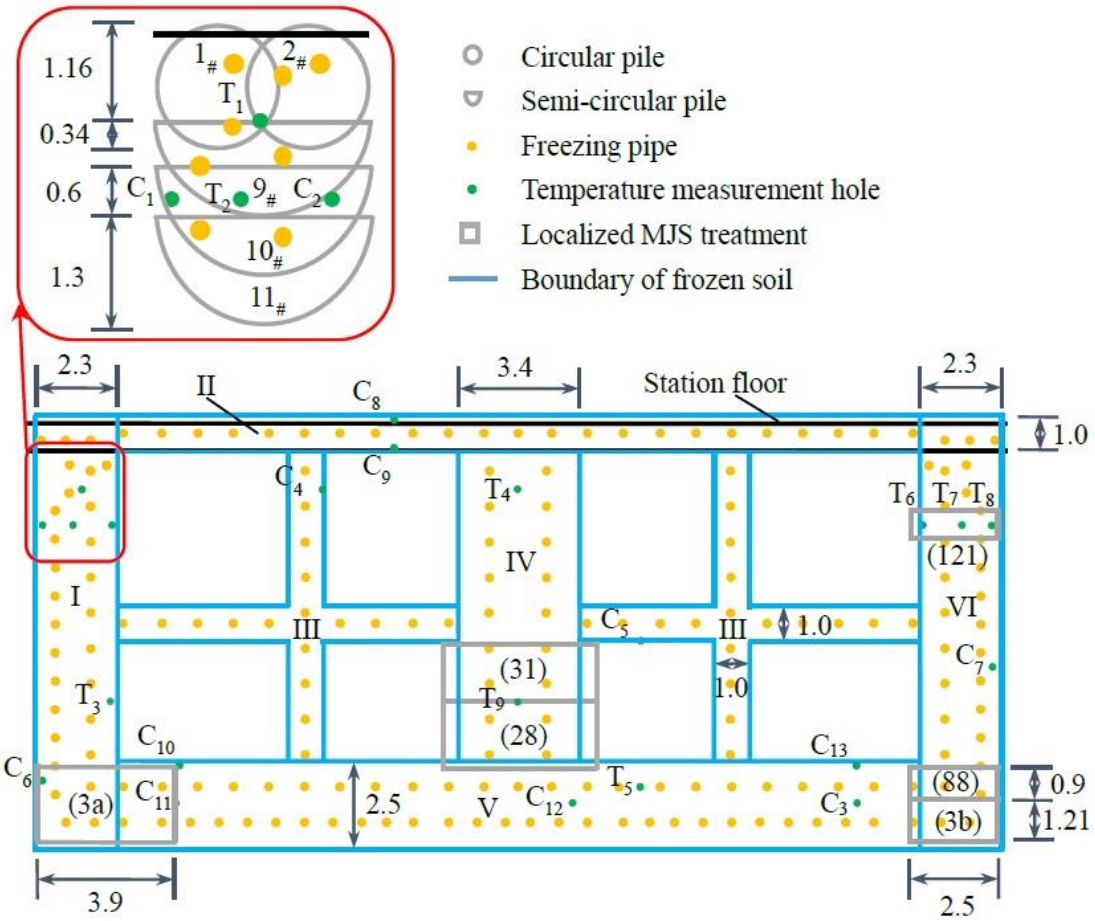

Fig. 2 Layout of MJS, freezing pipes, temperature measuring pipes, and designed frozen soil area (units: m)

2.2 Design of ground improvement

2.2.1 MJS treatment

The construction zone was partially reinforced using MJS as shown in Fig. 2. To reduce the frost heave and the subsequent thaw settlement, the area of frozen wall was set to be consistent with the MJS treatment area. Piles (i.e., MJS reinforced area in semi-circular shape) were created after the MJS treatment. To form a consecutive MJS reinforcement area, circular piles with a diameter of 1.5 m were constructed using MJS at the bottom of the existing station. The MJS treatment was made with a cement-soil mixing ratio of 55%. Besides, a total number of 84 semi-circular piles with a radius of 1.3 m were constructed with help of MJS. The center-to-center spacing between consecutive piles was 0.6 m as shown in Fig. 2. The MJS treatment of these semi-circular piles was made at a cement-soil mixing ratio of 60%. A total number of 92 horizontal MJS piles were constructed to reinforce the ground before freezing. The MJS treatment was started on May 18th, 2020, and completed on Sep 22th, 2020.

2.2.2 AGF setup

The AGF was implemented after the MJS reinforcement. As shown in Fig. 2, a total number of 372 freezing pipes were installed along the axial direction of the tunnel. 58 freezing pipes, with a length of 3.0 m (i.e., 1.2 m in soil and 1.8 m in the diaphragm wall) were set to be beneath the existing station to form a closed frozen soil wall. The length of rest freezing pipes is between 13.5 ~ 18.65 m (1.8 m inside the diaphragm wall), freezing pipes are driven into the soil from both ends of the section, and the overlapping length of these freezing pipes is 2.0 m at the center. The layout of 186 AGF holes and 22 temperature measurement holes is also shown in Fig. 2. The blue and yellow dots denote the AGF holes and temperature measurement holes, respectively. The Φ108 × 8 mm low carbon steel seamless pipe (i.e., outside diameter of 108 mm and thickness of 8 mm) was used as the freezing pipes. The distance between the diaphragm wall and sidewall of Metro Line 10 was 1.2 m. The design thickness of the frozen soil walls at different locations is shown in Fig. 2. The excavation was initiated when the thickness of frozen soil wall met the requirement.

3. Numerical simulation

3.1 Build model

The temperature measurement was only made on part of section in the field. In addition to this on-site measurement, a numerical simulation was also conducted to characterize the temperature variation induced by MJS and AGF using ADINA

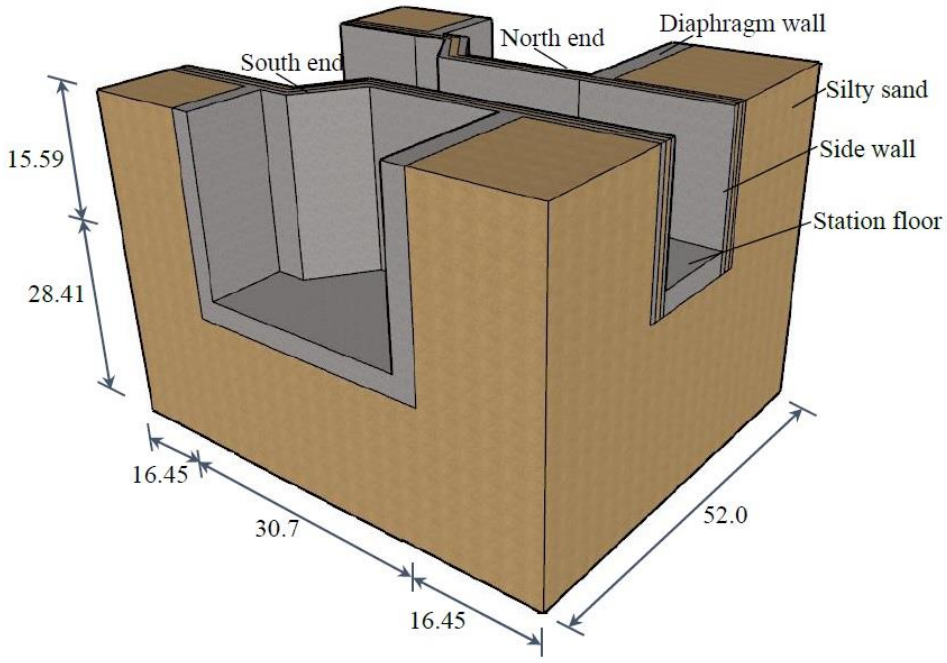

Fig. 3 Three-dimensional model of the ground improvement section (units: m)

software package. The size of the three-dimensional (3D) model is set to be consistent with that of the construction site, as shown in Fig. 3, 52.0 m parallel to the tunnel, 63.6 m in width, and 44.0 m in height. The thicknesses of the diaphragm wall and station floors are 1.8 and 1.0 m, respectively. In this model, the mesh size ranges from 0.1 m to 0.5 m. The principle of meshing is to have a smaller mesh in zones with highly non-uniform temperature distribution (e.g., MJS and AGF reinforcement area and its surroundings). The model is consisted of 28, 896, 873 elements.

3.2 Assumptions

To facilitate the numerical modeling , some assumptions were made as follows:

1. The temperature of soil is 21°C that is simplified to be uniform;
2. In the process of temperature variation, the boundary of the model is considered to be adiabatic;
3. The thermal properties of the same type of soil are isotropic under frozen or unfrozen state;
4. The influence of freezing pipe (i.e., steel pipe) is ignored since the wall thickness is much less than its diamerter and the thermal conductivity is relatively high.

3.3 Control equations

It is assumed that the material of the body obeys Fourier's law of heat conduction in each direction

$$q_x = -k_x \frac{\partial \theta}{\partial x}; \quad q_y = -k_y \frac{\partial \theta}{\partial y}; \quad q_z = -k_z \frac{\partial \theta}{\partial z} \tag{1}$$

q_x, q_y, q_z, = heat flux (heat flow conducted per unit area),
k_x, k_y, k_z, = thermal conductivity
θ = temperature.

Balance of heat flow in the interior of the body

$$\frac{\partial}{\partial x}\left(k_x \frac{\partial \theta}{\partial x}\right) + \frac{\partial}{\partial y}\left(k_y \frac{\partial \theta}{\partial y}\right) + \frac{\partial}{\partial z}\left(k_z \frac{\partial \theta}{\partial z}\right) = -q^B \tag{2}$$

q^B= the rate of heat generated per unit volume.

Convection boundary conditions

$$q^S = h(\theta_e - \theta^S) \tag{3}$$

Where h is the convection coefficient, θ_e the environmental temperature, and θ^S is the temperature of body surface.

Phase change: At a solid-liquid interface the latent heat is liberated (or absorbed) of the material from one phase to the other.

3.4 Thermal properties

The thermal properties of the on-situ soil are measured through a portable meter and the results are listed in the following table.

3.5 Temperature load

With the temperature recorded by the Nanjing meteorological station of the National Environmental Information Center (www.ncei.noaa.gov) which is the meteorological monitoring station nearest to the construction site, the hourly variation of atmospheric temperature during the implementation of MJS and AGF is presented in Fig. 4. This air temperature was applied as a

Table 1 Soil thermal properties

Properties	Unit	Silty sand	CSS	Concrete	Insulation
Density	kg/m^3	1910	2001	2500	35
Phase transition Temperature	°C	[-2,0]	[-2,0]	-	-
Thermal conductivity	Frozen（W/m.°C）	1.91	1.47	-	-
	Unfrozen（W/m.°C）	1.42	1.19	1.74	0.024
Heat capacity	Frozen（kJ/kg.°C）	1.25	1.01	-	-
	Unfrozen（kJ/kg.°C）	1.76	1.24	0.92	1.38
Water content		26.5%	32.4%		
Latent heat	10^8J/m^3	1.26	0.98	-	-

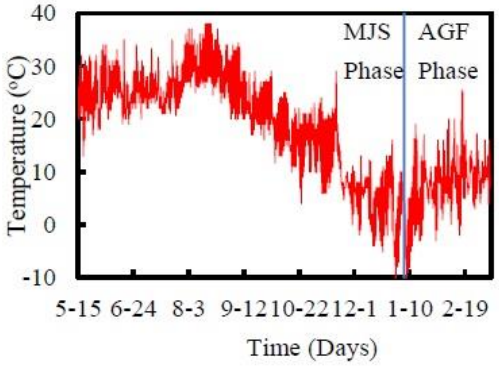

Fig. 4 Air temperature variation

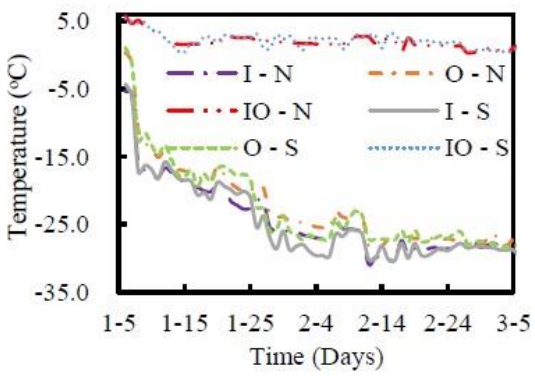

Fig. 5 Calcium chloride brine temperature variation

critical boundary condition. The soil temperature before MJS treatment is 21°C. The shape of MJS piles are equivalent to cuboid when the geometric model is established, and the MJS piles with similar construction time is assumed to start construction at the same time. The part of simplified MJS piles area and construction time are shown in the Fig. 2. The assumptions, governing equations, thermophysical properties, boundary conditions, and the hydration heat released per cubic meter of CSS released over time are consistent with that presented in Zhao *et al.* (2020). The schedule of the construction is shown in Fig. 2.

The temperature of the calcium chloride brine was monitored once per day during freezing. Fig. 5 shows the temperature variation at the inlet and outlet of the brine flow. The "I", and "O", in Fig. 5 respectively represent the inlet flow and outlet flow temperatures of brine. The "N" and "S" represent the temperatures at the south end and north end of the section. The "IO" represents the temperature difference between the inlet and outlet brine flow. The maximum temperature difference between the inlet flow and outlet flow after freezing for seven days is less than 3°C. The temperature difference between the inlet and outlet flow decreased over time.The temperature of the inlet brine flow and outlet brine flow both dropped to -25°C in approximately 20 days after the initiation of freezing. In the later stage, the brine temperature stabilized at approximately -28°C. In simulation, the brine temperature of one day is set to be consistent with the average of the inlet and outlet brine temperatures of the corresponding day. The hydration heat released during CSS curing was presented in Zhao *et al.* (2020).

4. Results and discussion

4.1 Field monitoring

4.1.1 Temperature monitoring method and arrangement of temperature measuring holes

The 44 holes, green dot as shown in Fig. 2 at MJS + AGF reinforcement area, were the locations where the soil temperature was measured during the application of MJS and AGF. It's worth noting that these holes are axisymmetric and only those in the south end are visible in Fig. 2. The thermocouples, at accuracy of 0.1°C, were employed to monitor soil temperature variation. Calibration was conducted in the laboratory before filed application. The temperature readings were recorded once a day.

4.1.2 Temperature variation after MJS treatment

The equipment for the MJS treatment is shown in Fig. 6(a). To evaluate the influence of CSS hydration heat on ground temperature, 18 holes with 70 temperature sensors were made. The tube and wire for the thermocouples are shown in Fig. 6(b). The timing for the initiation of temperature monitoring in different temperature measuring holes is shown in Fig. 7. Since freezing in the project was started on Jan. 5th, 2021, and the temperature monitoring of data of soil influenced only by MJS hydration heat ended on Jan. 4th, 2021.

(a) MJS equipment

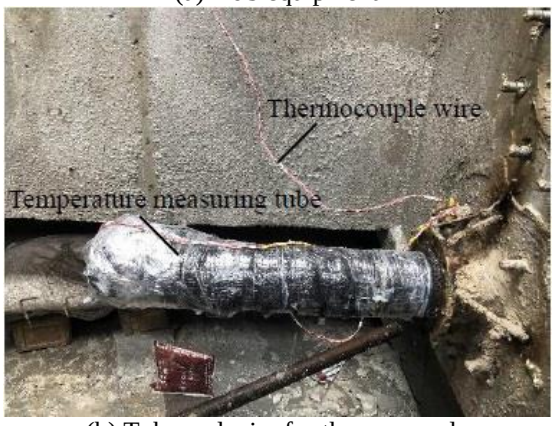

(b) Tube and wire for thermocouple

Fig. 6 Schematic diagram in the MJS phase

Fig. 7 shows the ground temperature variation of some measuring temperature points with time after the MJS treatment. Using '$T_{1\text{-}2}$ (3.0)' as an example, where "T_1" (i.e., T was used to monitor the soil temperature during MJS and AGF.) represents the temperature measuring hole in Fig. 2, "2" represents the second thermocouple in this hole, "3.0" represents the buried depth of this thermocouple is 3.0 m in the ground. Note that some of the thermocouples in T_1, T_7 and T_8 as shown in Fig. 2 were unintentionally damaged during the installation of freezing pipes. The temperature measurement holes could not be made in the ground right after the MJS treatment. This was the exact reason why the temperature variation was not available at the early stage. The highest temperature occured at the beginning of the temperature monitoring, since there is only a little rising stage of soil temperature for most of the hydration heat has been released within three days after MJS construction, as shown in Fig. 4 (Zhao *et al.* 2020). With time, the ground temperature continuously decreased. As shown in Fig. 7, comparing the temperature at different depths in the same hole, ground temperature increased with an increase of depth. This was because of a lower depth was beneficial for the quick release of heat through thermal convection since it's closer to the asmophere. Note that the temperatures at $T_{1\text{-}1}$, $T_{2\text{-}1}$, and $T_{6\text{-}1}$ were very close to 15ºC (which was lower than the initial soil temperature of 21ºC) before freezing. This was because the air temperature significantly decreased in winter according to Fig. 4.

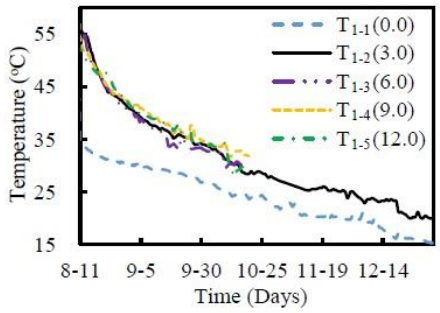

(a)

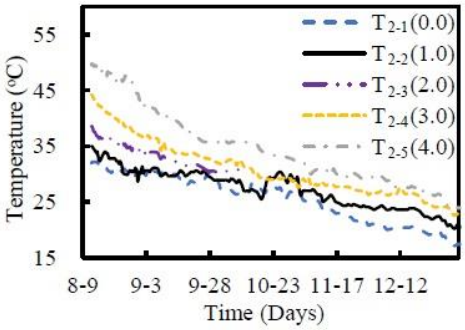

(b)

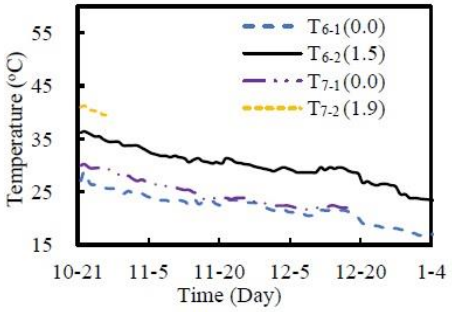

(c)

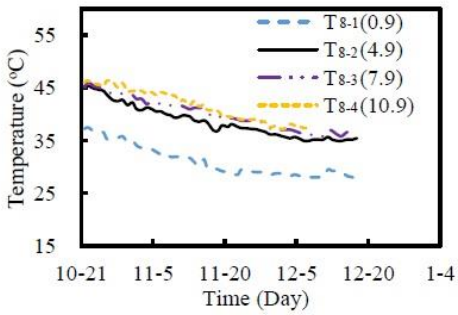

(d)

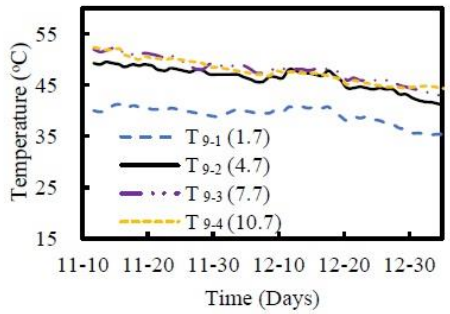

(e)

Fig. 7 Temperature variation after MJS treatment in 2020

(a) Equipments for freezing

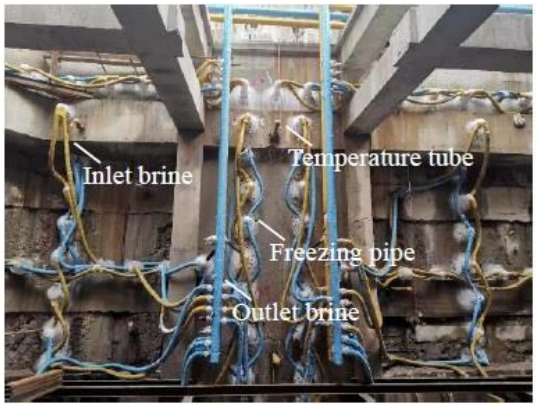

(b) Freezing

Fig. 8 AGF system

In Fig. 2, the temperature measurement hole T_1 is next to $1_{\#}$, $2_{\#}$, $9_{\#}$ MJS piles and T_2 is mainly affected by $9_{\#}$, $10_{\#}$, and $11_{\#}$ piles of MJS. The time spans from the completion of $1_{\#}$, $2_{\#}$, $9_{\#}$, $10_{\#}$, and $11_{\#}$ MJS piles to the beginning of freezing are 161, 165, 169, 172, and 174 days, respectively. The soil temperature at T_1 and T_2 were very close to the initial ground temperature (i.e., 21ºC) before freezing because most of the heat released during curing gradually dissipated to surrounding soil with time. The temperature at T_7 is higher than those at T_6 and T_8 before freezing. The MJS treatment around T_9 was three months later than that of the MJS piles around T_7, the temperature of T_9 is higher than that of T_7 on Dec 14th, 2020 which is reasonable since the width of soil treated by MJS around T_9 is 1.6 times that around T_7.

4.1.3 Temperature variation after AGF

The main purpose of continuous on-site temperature monitoring is to determine whether the thickness of frozen soil wall metts the requirement or not before excavation. When the thickness of frozen zone is less than the designed value, the frozen zone will not be able to resist the stress induced by excavation. A too large thickness might damage the excavation boundary, increase the difficulty of tunnel construction, and cause higher costs. The drilling for freezing pipes and equipment installation (shown as in Fig. 8(a)) started on Aug 7th, 2020 and ended on Jan 4 th, 2021. On Jan 5th, 2021, the freezing was initiated as shown in Fig. 8(b).

The ground temperature variation recorded during freezing using thermocouples was plotted in Fig. 9. The ground temperature quickly decreased before reaching the freezing point, gradually decreased with time, and then stabilized at the later stage of freezing. The reason for this is that the temperature difference between the brine and soil treated by MJS is significant at the early freezing stage, and this difference gradually decreases with the progression of freezing. When the soil temperature reached the freezing temperature (i.e. -0.31ºC), the water-ice phase change and the associated release of latent heat delayed the decreasing of soil temperature. The temperature dropped rapidly around 2/14. This was because the temperature of the calcium chloride brine from 2/8 to 2/12 was higher than that after 2/12. The temperature of the most temperature measuring point drops rapidly around 2/14 day since there is a certain distance between the temperature measuring point and the freezing pipes.

The ground temperature near the diaphragm wall is always the lowest in the same temperature measuring hole. The further the distance between a temperature measuring point and the end section, the more time the temperature at the temperature measuring point requires to reach a frozen state. This illustrates that thermal convection has a significant impact on the formation of frozen soil near the diaphragm wall when AGF is applied. This temperature variation during freezing is different from that without an MJS treatment before freezing. Freezing reinforcement projects without the effect of hydration heat, usually, the area near the diaphragm wall under the influence of thermal convection is the weak frozen section whether in winter or summer. For example, horizontal freezing technology was adopted to reinforce the soil surrounding a single lane service tunnel which was constructed to improve passenger transport capacity at Shanghai Pudong International Airport (Zhou *et al*. 2021). AGF was chosen as an auxiliary measure in the project of the tunnel beneath a block of historical buildings in the German town Fürth (Pimentel *et al.* 2012).

The temperature variations are different from each other during freezing since the location and the initial soil temperature affected by the CSS hydration heat are different before freezing. As illustrated in Fig. 9(c), the soil temperature at C_3 was higher than that at C_{13} before freezing, the cooling rate at C_{13} is lower than that at C_3 at the beginning of freezing, and the temperature at C_3 is lower than that at C_{13} at the later period of freezing. This is because C_3 is affected by two rows of freezing pipes, and C_{13} is only affected by one, as shown in Fig. 2. The temperature at T_9 is higher than that at T_4 before freezing, the temperature difference between T_4 and T_9 gradually decreases with time, and the temperatures at T_4 and T_9 are similar at the end of freezing. Since the distance between T_4 and freezing pipes is the same as that between T_9 and freezing pipes. The temperature variation of $C_{1'}$ in the north end and that of C_1 in the south end were compared, as illustrated in Figs. 9(a) and 9(e). It is found that the temperature variation in the same position of the north and south ends are practically identical, and thus the temperature variation in the north end is not analyzed.

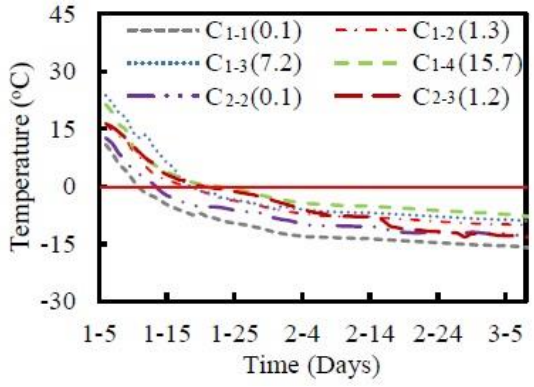

(a)

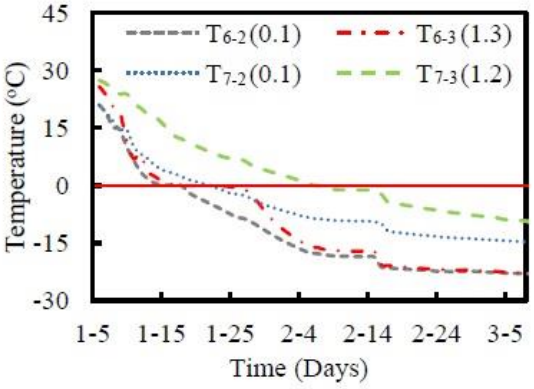

(b)

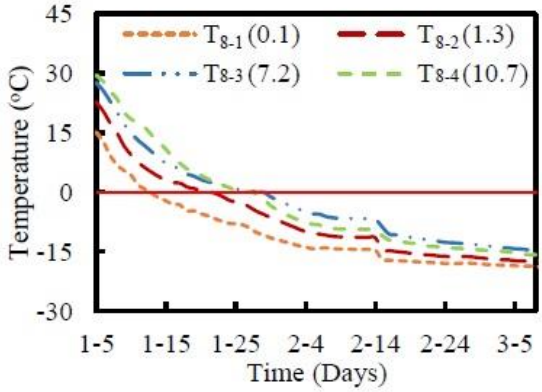

(c)

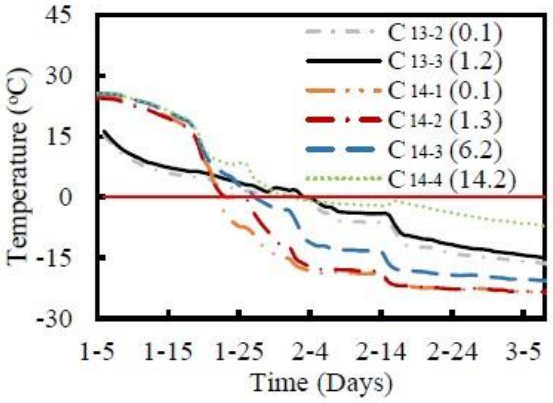

(d)

Fig. 9 Temperature variations with time

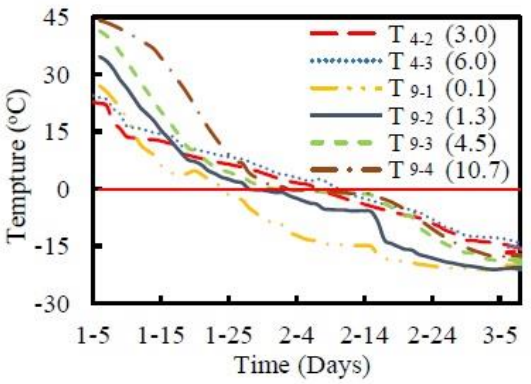

(e)

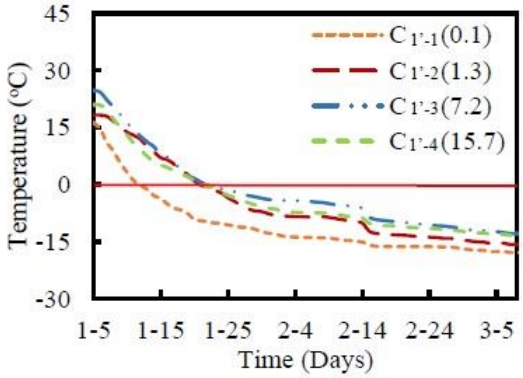

(f)

Fig. 9 Continued

4.2 Simulation results

4.2.1 Hydration heat induced temperature variation

Fig. 10 shows the CSS temperature distributions caused by hydration heat obtained from the numerical simulation at different times (i.e., day 50, 100, 150, and 234 after MJS starts construction). Since the CSS section is symmetric, the temperature distribution at only one end section is visible. With time, the heat released by the cemented soil is gradually transferred from the high- to low-temperature zone, and the zone under the influence of hydration heat is gradually expanded. On the day 126, the construction of all MJS piles was completed, the newly released heat is getting less and less, and all the soil temperature differences at different locations inside the cemented soil began to decrease with time. Therefore, the soil temperature difference is significant on the surface of CSS on the day 50 and day 100. The temperature difference was insignificant on day 234, and the soil temperature on the surface of CSS dropped to the initial ground temperature. Since thermal convection at the end section continuously takes away heat from the soil near the end section, the soil temperature at the top and end sections is significantly lower than that at the middle section.

In the first 12 days after the MJS treatment, the ground temperature in areas of (3a) and (3b) (see Fig. 2) are not affected by other MJS reinforcement areas. Therefore, (3a) and (3b) are selected as examples to analyze the influence

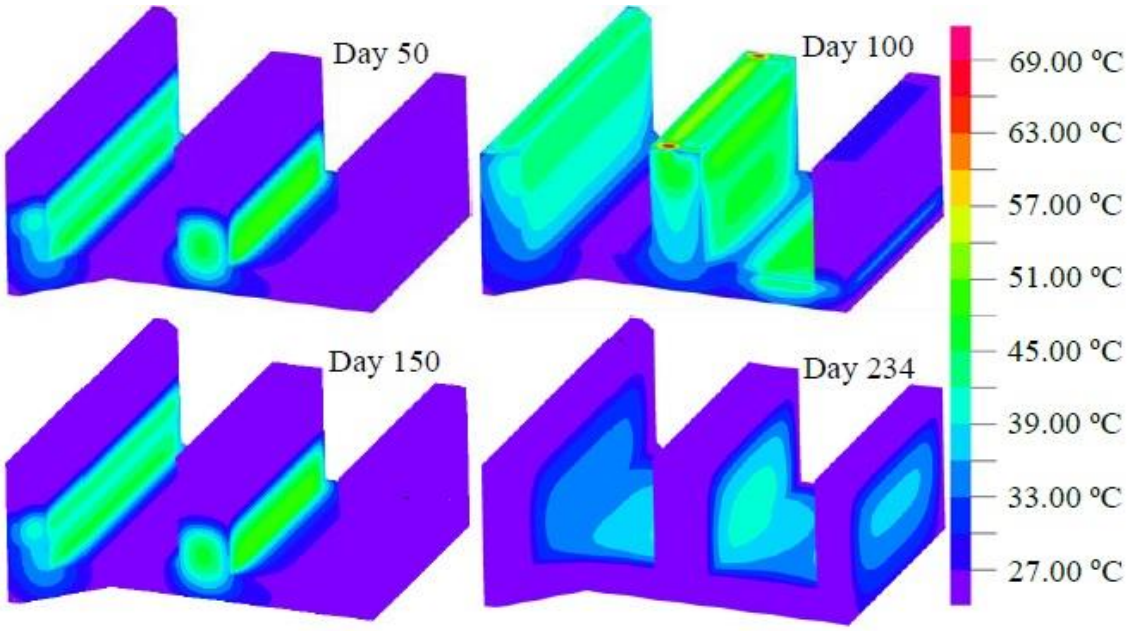

Fig. 10 The temperature field of CSS is induced by CSS hydration heat

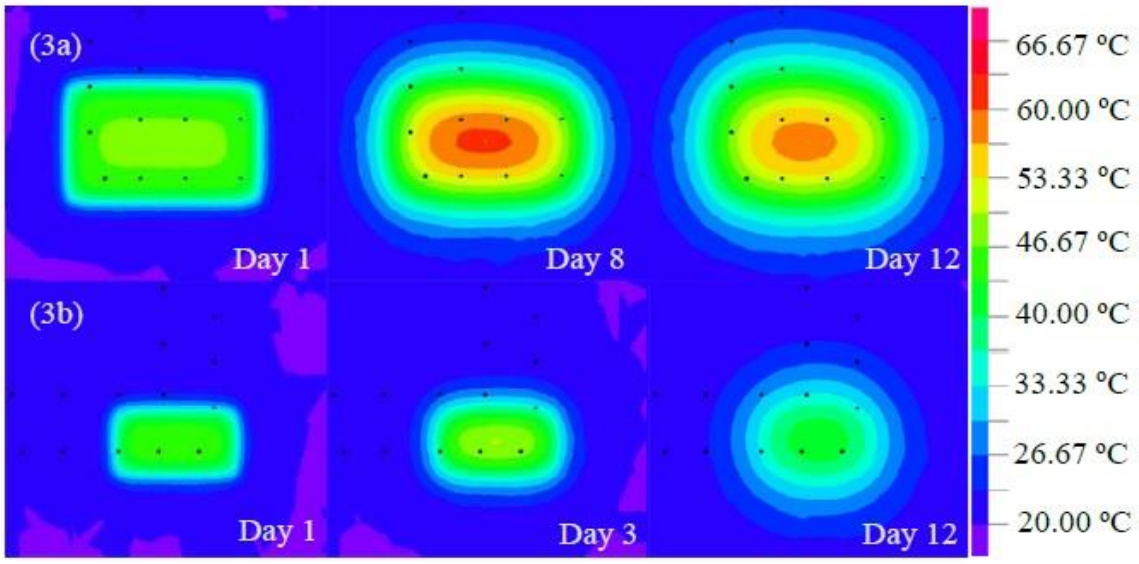

Fig. 11 Temperature distribution in the middle section of (3a) and (3b) is induced by hydration heat at different days

of MJS treatment on ground temperature. The sections of (3a) and (3b) is 3900×2110 mm and 2500×1210 mm, respectively. Fig. 11 shows the color map of soil temperature distribution of (3a) and (3b) areas at the middle section at the end of days 3, 5, 8, and 12 after MJS treatment. To be specific, the highest temperature, such as 47.15°C and 45.64°C at the end of day 1, and 58.31°C and 41.71°C at the end of day 12, is always found at the center of 3(a) and 3(b), respectively. The highest soil temperature is 60.85°C and 49.37°C within 12 days after MJS treatment at (3a) and (3b), which occurred on days 8 and 3, respectively. Therefore, the larger the area of MJS treatment area is, the higher the soil temperature, and the later the highest temperature occurs.

4.2.2 AGF induced temperature variation

The temperature field at the end of day 234 after the MJS treatment was used as the initial temperature field for the simulation of ground temperature under the influence of AGF. The end sections (Fig. 3) are exposed to atmosphere, and the freezing process is considerably affected by convection. To reduce the active freezing time (AFT, time for thickness of frozen soil wall to reach the required thickness), thermal insulation (polyurethane) is applied at the end sections during freezing. The density, thermal conductivity, thickness, and specific heat capacity of polyurethane are the same as those in elsewhere (Zhao *et al*. 2020). It is impractical to set an insulation layer on the floor of the existing station, as a result, more freezing pipes were

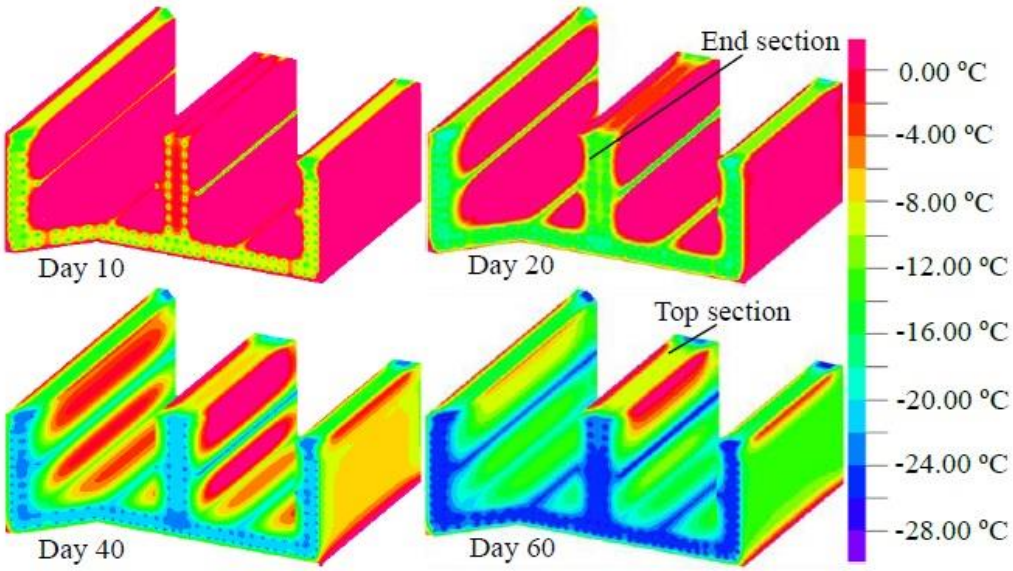

Fig. 12 Typical temperature distribution of CSS caused by AGF on different days

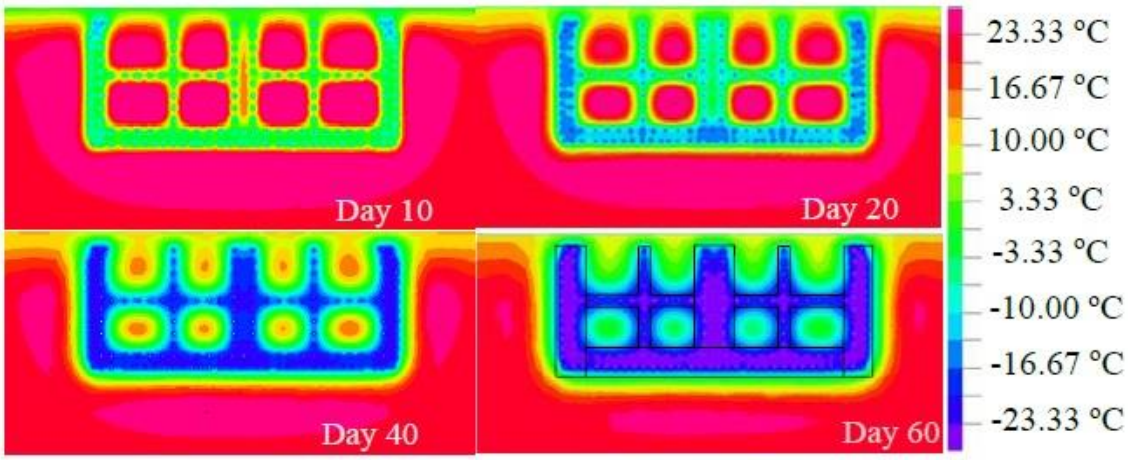

Fig. 13 Temperature distribution of AGF at the middle section

added below the floor before freezing, as shown in Fig. 2.

Fig. 12 shows the temperature distribution of CSS at the end of days 10, 20, 40, and 60 caused by AGF obtained through simulation. After 10-day freezing process, the soil temperature at middle section is slightly higher than those at both sides at the end sections. After freezing for 20 days, the temperature at the end sections of CSS is below 0°C. After freezing for 60 days, most of the CSS temperature is below 0°C. Note that the soil temperature at the end sections is always lower than that at the middle section which implies the weak zone is located at the middle section. The major reason is that the soil temperature at the middle section is higher than that at the end section before freezing, as shown in Fig. 12. Another reason is that the mean atmospheric temperature during freezing is about 7.3°C, which is close to the mean winter air temperature of 5.9°C in the past years. The lower atmospheric temperature is beneficial to the formation of frozen soil walls at end sections during freezing.

According to the above simulation results, more attention should be paid to the weak zone at the middle section. Fig. 13 shows the soil temperature distribution based on the hydration heat of CSS after freezing for 10, 20, 40, and 60 days at the middle section. With continuous freezing, the area of the frozen soil zone increases, and the soil temperature decreases in this zone. The freezing front (i.e., 0°C isotherm) experiences a fast first and then slow development. After freezing for 10 days, the soil temperature around the freezing pipes dropped to 0°C below. However, the temperature around cemented soil is still above 23°C, which is due to the hydration heat resulted in an increase of the initial soil temperature before freezing. After freezing for 20 days, all frozen soil piles have been intersected. After freezing for 40 days, only a small part of soil temperature is higher than 23°C. After freezing for 60 days, the soil temperature within the area that enclosed by the black dotted line in Fig. 13 (Day 60) represents the requirement of frozen soil wall the designed requirements of frozen soil is below 0°C.

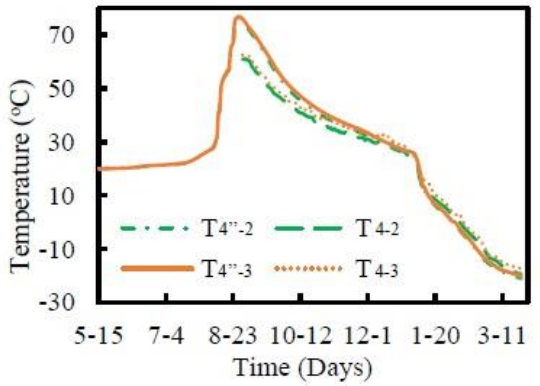

(a)

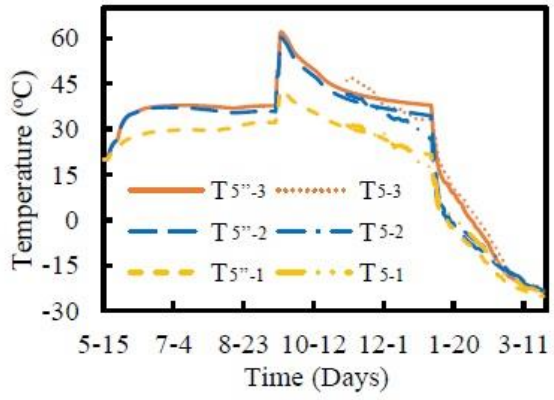

(b)

Fig. 14 Comparison between numerical simulation and measurement result

4.2.3 Effect of AGF timing on AFT after MJS treatment

A reasonable start-freezing time is of great significance for energy conservation. To evaluate the influence of AGF timing after MJS treatment, the soil temperature distribution at the end of 60, 70, 80, 90, 100, 110, and 120 days after the MJS treatment are utilized as the initial soil temperature for AGF. The time for the numerical simulation to reach the required thickness of frozen soil wall can be seen in the temperature field color map. According to the simulation result, the difference in AFT is only 2 days between two cases which are AGF is respectively initiated at the end of day 60 and day 120 after the MJS treatment. In other words, the influence of the timing for the initiation of AGF is insignificant on AFT. This phenomenon is mainly because of the fact that the heat loss due to thermal convection is insignificant.

4.3 Comparison between numerical simulation and field measurement

In addition to the above analysis of measured and simulated data, comparisons were made between numerical simulation and field measurement result to verify the rationality of the numerical simulation. Using T_4 (at depths of 2 m and 3 m), and T_5 (at depths of 1 m, 3 m, and 6 m) as examples, the soil temperature variation obtained from the on-site measurement and simulation during MJS and AGF processes are plotted in Fig. 14 ($T_{4"-2}$ represents the temperature at T_{4-2} obtained by simulation). The temperature variation from the numerical simulation matches well with the on-site measurement result. The average difference in temperatures between the numerical simulation and field measurement at all measuring points is approximately 3°C. The maximum temperature difference between the numerical simulation and the measured data is 14.31°C of T_{4-2}, and 7.21°C of T_{5-2} during hydration heat and freezing process (Fig. 14).

Besides the ground temperature, a comparison was made on AFT obtained based upon simulation and on-site measurement. As depicted in Fig. 2, the entire section is divided into I, II, III, IV, V, and VI areas. The required frozen soil wall thickness in each area is calculated using the measured data according to the formula, Eqs. (4) and (5), proposed by Cui (2003).

$$r_2 = \frac{r}{T_1} T \tag{4}$$

Where r_2 is the radius of frozen soil column (m), T_1 is time that temperature of measuring point reaches 0°C (Days), T is freezing time (Days), and r is the distance between the freezing pipe and the temperature measurement hole (m).

$$E = L + 2\sqrt{r_2^{\,2} - \frac{l_2}{4}} \tag{5}$$

Where E is frozen soil wall (m), L is spacing of freezing pipe rows (m), r_2 is the freezing pipe spacing (m). According to the measurement, the corresponding calculated parameters and results are listed in Table 2.

The AFT of each frozen soil area based on measurement and simulation results are listed in Table 2 (i.e., T' is AFT based on on-site measurement). Among six areas, the influence of thermal convection on zone II is the most significant by thermal convection (i.e., Both end section and top section is close to concrete wall) and is the last area that reaches the thickness of the designed frozen soil wall. The required thickness of the frozen soil wall in area III is small and is less affected by thermal convection and hydration heat. It is worth mentioning that the AFT of area III is much less than the other areas.

Accordint to Table 2, after a 63-day freezing process, the thickness of frozen soil wall can satisfy the requirement in all six areas. The numerical simulation results indicates that a 60-day freezing process is sufficient for all six area. For each area, the specific requirement of AFT is different from each other. This is confirmed by both simulation and on-site measuremnet results. In terms of AFT, a slight difference exists between the simulation and measurement results. This difference was attributed to the following reasons: (1) Air temperature recorded by the local meteorological station was used as a critical boundary condition in the simulation to represent the on-site air temperature.

However, the on-site air temperature was not only dependent on the air temperature but also the artificial freezing system, the construction activities, etc; (2) The

Table 2 Time required to meet the designed thickness of different frozen zones

Parameters / Frozen area	E	L	l_2	r_2	r	T_1	Measuring point	T	T'
I	2.3	0.8	1.0	0.9	0.445	25	C5-3 (7.2)	52	48
II	1.0	0	1.1	0.74	0.711	60	C8-3 (1.2)	63	60
III	1.0	0	1.0	0.71	0.673	30	C17-3 (1.2)	32	33
IV	3.4	1.6	1.0	1.03	0.673	30	C17-3 (1.2)	46	46
V	2.5	0.9	1.0	0.94	0.78	38	C10'-4 (12.2)	46	50
VI	2.3	0.8	1.0	0.9	0.75	43	T3-2 (3)	51	52

location of freezing pipes and temperature measurement holes were idealistic in the numerical simulation. Because of construction error, a deviation in angle ranging from -2.0 to 2.3 was recorded for freezing pipes and temperature measuring holes; (3) The reinforcement area and timing of MJS treatment were simplified in the simulation. The MJS piles were constructed one by one. However, in the simulation, the construction for some MJS piles (i.e., with similar construction time) was accomplished at the same time; (4) The average of the brine temperatures at the inlet and outlet of the freezing pipes was used as the representative brine temperature in the numerical simulation; (5) The soil might not be uniformly distributed.

A difference between the measurement and numerical simulation results always exists since the complexity of the construction process and boundary conditions of the project. However, a numerical simulation is still strongly recommended for the following reasons: The predicted active freezing time was 3 days (i.e., only about 5%) longer than the actual active freezing time. Only limited temperature measurement holes can be made in the field. A numerical simulation can better reflect the overall soil temperature distribution instead of the soil temperature in several holes. The overall temperature distribution is essential for the design of an efficient and economical freezing system and provide reference for similar projects. In addition to soil temperature prediction, a numerical simulation is also beneficial to elucidate the progression of the temperature field induced by hydration heat and freezing.

5. Conclusions

In this paper, the influence of hydration heat and artifical freezing on the ground temperature was analyzed through on-site measurement and numerical simulation based on an existing project. Several conclusions were drawn as follows:

- According to the on-site measurement result, the hydration heat from the MJS treatment resulted in a significant increase of ground temperature. The ground temperature then declined rapidly and gradually stabilized before freezing. The soil temperature in the same measuring hole increases with the depth due to the influence of hydration heat and convection. It takes 63 days to meet the requirement on frozen wall thickness. The weak area is located in the middle of the project and near the station floor.
- The numerical simulation indicates that the larger the reinforcement range of the MJS area, the higher the maximum temperature of soil caused by hydration heat, and the more time required by the occurence of the highest temperature. After freezing for 20 days, capacity closed frozen soil wall was generated. After the MJS treatment, the influence of the timing for the initiation of AGF is insignificant on AFT.
- The simulation result matches well with the on-site measurement. An average difference of 3ºC was identified between numerical simulation and field measurement data. This difference is mainly attributed to the assumptions made to simplify the simulation, non-uniformity in brine temperature, and construction error, etc.

Acknowledgments

The research work herein was supported by the National Natural Science Foundation of China (No.52178337), the China Scholarship Council Project (Grant N0.202108320283), and the National First-class Disciplines.

References

Casini, F., Gens, A., Olivella, S. and Viggiani, M.B.G. (2016), "Artificial ground freezing of a volcanic ash: laboratory tests and modeling", *Environ. Geotech.*, **3**(3), 141-154. https://doi.org/10.1680/envgeo.14.00004.

Chen, C. and Yang, P. (2021), "Study on the prevention and control for shield tail leakage of large-diameter river-crossing tunnel at high hydraulic pressure", *J. For. Eng*., **6**(1), 155-162. (in Chinese).

Chen, R.P., Lin, X.T., Kang, X., Zhong, Z.Q., Liu, Y., Zhang, P. and Wu, H.N. (2018), "Deformation and stress characteristics of existing twin tunnels induced by close-distance EPBS under-crossing", *Tunn. Undergr. Sp. Tech*., **82,** 468-481. https://doi.org/10.1016/j.tust.2018.08.059.

Cui, Y.L. (2003), Well Construction Engineering Manual, Coal Industry Press, Beijing, China.

Fan, W.H. and Yang, P. (2019), "Ground temperature

characteristics during artificial freezing around a subway cross passage", *Trans. Geotech.*, **20**, 100250. https://doi.org/10.1016/j.trgeo.2019.100250.

Fu, Y., Hu, J. and Wu, Y.W. (2021), "Finite element study on temperature field of subway connection aisle construction via artificial ground freezing method", *Cold Reg. Sci. Technol*., **189**, 103327. https://doi.org/10.1016/j.coldregions.2021.103327.

Hu, Y., Lei, H.Y., Zheng, G., Shi, L., Zhang, T.Q., Shen, Z.C. and Jia. R. (2021), "Assessing the deformation response of double-track overlapped tunnels using numerical simulation and field monitoring", *J. Rock Mec. Geotech. Eng.*, **14**(2), 436-447. https://doi.org/10.1016/j.jrmge.2021.07.003.

Huang, X.W., Yao, Z.S., Cai, H.B., Li, X.W. and Chen, H.Q. (2021), "Performance evaluation of coaxial borehole heat exchangers considering ground non-uniformity based on analytical solutions", *Int. J. Therm. Sci.*, **170**, 107162. https://doi.org/10.1016/j.ijthermalsci.2021.107162.

Huang, S.B., Guo, Y.L., Liu, Y.Z., Ke, L.H., Liu, G.F. and Cheng, C. (2018), "Study on the influence of water flow on temperature around freeze pipes and its distribution optimization during artificial ground freezing", *App. Therm. Eng.*, **135**(1), 435-445. https://doi.org/10.1016/j.applthermaleng.2018.02.090.

Jin, H., Go, G.H., Ryu, B.H. and Lee, J. (2021), "Experimental and numerical investigation of closure time artificial ground freezing with vertical flow", *Geomech. Eng*., **27**(5), 433-445. https://org/10.12989/gae.2021.27.5.433.

Lackner, R., Amon, A. and Lagger, H. (2005), "Artificial ground freezing of fully saturated soil: thermal problem", *J. Eng. Mec*., **131**(2), 211-220. https://doi.org/10.1061/(ASCE)0733-9399(2005)131:2(211).

Levin, L., Golovatyi, I., Zaitsev, A., Pugin, A. and Semin, M. (2021), "Thermal monitoring of frozen wall thawing after artificial ground freezing: Case study of Petrikov Potash Mine", *Tunn. Undergr. Sp. Tech*., **107**, 103685. https://doi.org/10.1016/j.tust.2020.103685.

Li, K.Q., Li, D.Q. and Liu, Y. (2020), "Meso-scale investigations on the effective thermal conductivity of multi-phase materials using the finite element method", *Int. J. Heat Mass. Transf*., **151**, 119383. https://doi.org/10.1016/j.ijheatmasstransfer.2020.119383.

Li, K.Q., Miao, Z., Li, D.Q. and Liu, Y. (2022), "Effect of mesoscale internal structure on effective thermal conductivity of anisotropic geomaterials", *Acta Geotech.*, **17**(8), 3553-3566. https://doi.org/10.1007/s11440-022-01458-z.

Liu, J.G., Maa, B.S. and Cheng, Y. (2018), "Design of the Gongbei tunnel using a very large cross-section pipe-roof and soil freezing method", *Tunn. Undergr. Sp. Tech*., **72**, 28-40. https://doi.org/10.1016/j.tust.2017.11.012.

Liu, J.W., Zhang, Y.X., Yuan, M.Q., Zhao, Y.D. and Yang, J.S. (2022), "Determining the cause of tunnel damages during tunneling in silty clay", *Eng. Fail. Anal.*, **137,** 106156. https://doi.org/10.1016/j.engfailanal.2022.106156.

Marwan, A., Zhou, M.M., Abdelrehim, M.Z. and Meschke, G. (2016), "Optimization of artificial ground freezing in tunneling in the presence of seepage flow", *Comput. Geotech*., **75**, 112-125. https://doi.org/10.1016/j.compgeo.2016.01.004.

Pimentel, E., Papakonstantinou, S. and Anagnostou, G. (2012), "Numerical interpretation of temperature distributions from three ground freezing applications in urban tunneling", *Tunn. Undergr. Sp. Tech*., **28**, 57-69. https://doi.org/10.1016/j.tust. 2011.09.005.

Qi, W.Q., Yang, Z.Y., Jiang, Y.S., Yang, X., Shao, X.K. and An, H.B. (2022), "Investigation on ground displacements induced by excavation of overlapping twin shield tunnels", *Geomech. Eng.*, **28**(5), 531-546. https://doi.org/10.12989/gae.2022.28.5.531.

Russo, G., Corbo, A., Cavuoto, F. and Autuori, S. (2015), "Artificial ground freezing to excavate a tunnel in sandy soil. Measurements and back analysis", *Tunn. Undergr. Sp. Tech.*, **50**, 226-238. https://doi.org/10.1016/j.tust. 2015.07.008.

Shi, Y.F., Fu, J.Y., Yang, J.S., Xu, C.J. and Geng, D.G. (2017), "Performance evaluation of long pipe roof for tunneling below existing highway based on field tests and numerical analysis: case study", *Int. J. Géoméch*., **17**(9), 04017054. https://doi.org/10.1061/(ASCE)GM. 1943-5622.0000933.

Tonon, F. (2011), "ADECO full-face tunnel excavation of two 260 m^2 tubes in clays with sub-horizontal jet-grouting under minimal urban cover", *Tunn. Undergr. Sp. Tech.*, **26**(2), 253-266. https://doi.org/10.1016/j.tust.2010.09.006.

Tounsi, H., Rouabhi, A. and Jahangir, E. (2020), "Thermo-hydro-mechanical modeling of artificial ground freezing taking into account the salinity of the saturating fluid", *Comput. Geotech*., **119**, 103382. https://doi.org/10.1016/j.compgeo.2019.103382.

Vasilyeva, M., Stepanov, S., Spiridonov, D. and Vasil'ev, V. (2019), "Multiscale finite element method for heat transfer problem during artificial ground freezing", *J. Comput. Appl. Math*., **371**, 112665. https://doi.org/10.1016/j.cam.2019.112605.

Vitel, M., Rouabhi, A. and Tijani, M. (2015), "Modeling heat transfer between a freeze pipe and the surrounding ground during artificial ground freezing activities", *Comput. Geotech.*, **63**, 99-111. https://doi.org/10.1016/j.compgeo.2014.08. 004.

Wang, C., Han, J.T., Kim, S.K. and Jang, Y.E. (2021), "A novel preloading method for foundation underpinning for the remodeling of an existing building", *Geomech. Eng*., **24**(1), 29-42. https://doi.org/10.12989/gae.2021.24.1.029.

Yan, L., Wang, G., Chen, M., Yue, K.F. and Li, Q.N. (2018), "Experimental and application study on underpinning engineering of bridge pile foundation", *Adv. Civ. Eng*., **2018**, 1-13. https://doi.org/10.1155/2018/5758325.

Yang, P., Zhao, J.L. and Li, L. (2021), "An artificial freezing technique to facilitate shield tail brush replacement under high pore-water pressure using liquid nitrogen", *KSCE J. Civ. Eng.*, **25**(4), 1504-1514. https://doi.org/10.1007/s12205-021-0936-6.

Zhang, P., Liu, Y., Kang, X., Zhong, K. and Chen, R.P. (2018), "Application of horizontal MJS piles in tunneling beneath existing twin tunnels", *Proceedings of the 2nd International Symposium on Asia Urban GeoEngineering*. Springer Singapore. Singapore.

Zhao, J.L., Yang, P. and Li, L. (2020), "Investigating influence of metro jet system hydration heat on artificial ground freezing using numerical analysis", *KSCE J. Civ. Eng*., **25**(2), 724-734. https://doi.org/10.1007/s12205-020-5407-y.

Zhou, J., Zhao, W.Q. and Tang, Y.Q. (2021), "Practical prediction method on frost heave of soft clay in artificial ground freezing with field experiment", *Tunn. Undergr. Sp. Tech*., **107**, 103647. https://doi.org/10.1016/j.tust.2020.103647.

IC